Pulsations of a coated microbubble – Steady pulsations, transient break-up & effect of nearby surfaces

K. Efthymiou, K. Tsiglifis & N. Pelekasis

Laboratory of Fluid Mechanics and Turbomachinery

Department of Mechanical Engineering

University of Thessaly, Volos, GREECE

Funding: "ARISTEIA I" Program, Greek Ministry of Education

European Union
European Social Fund

OPERATIONAL PROGRAMME
EDUCATION AND LIFELONG LEARNING
investing in knowledge society
MINISTRY OF EDUCATION & RELIGIOUS AFFAIRS
MANAGING AUTHORITY

NSRF 2007-2013
programme for development
EUROPEAN SOCIAL FUND

Co-financed by Greece and the European Union

5th BIFD International Symposium, Haifa, Israel, 8-11 July 2013

Microbubbles (Contrast Agents)

- Bubbles surrounded by an elastic membrane for stability
- Low density internal gas that is soluble in blood
- Diameter from 1 to 10 μm
- Polymer, lipid or protein (e.g. albumin) monolayer shell of thickness from 1 to 30 nm

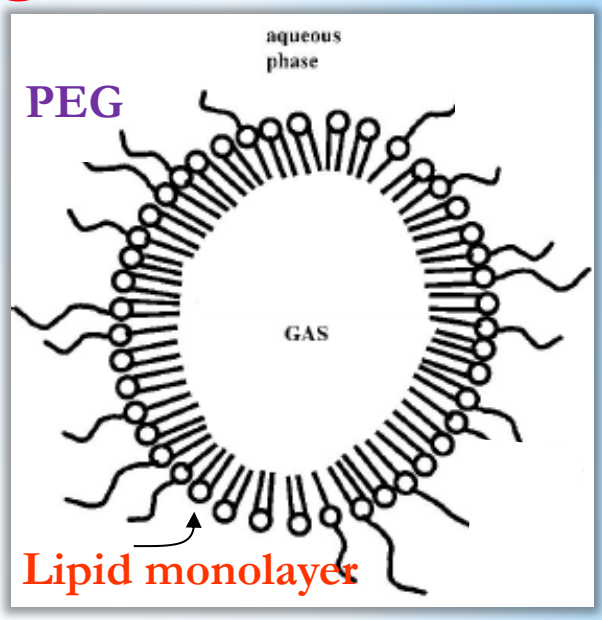

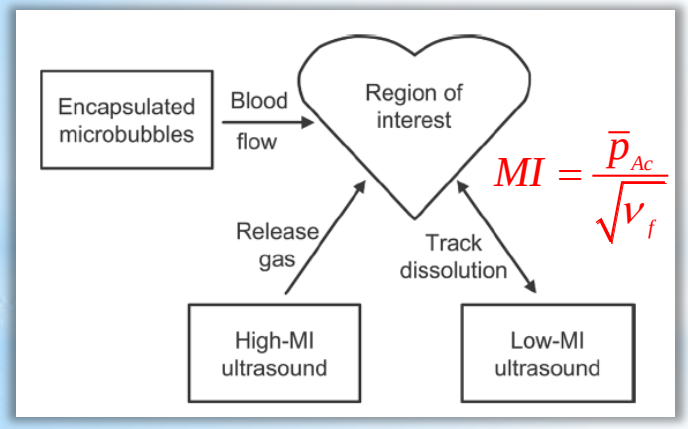

Contrast enhanced perfusion imaging, via a sequence of low and high Mechanical Index (MI) ultrasound pulses

Motivation

- Contrast perfusion imaging ⇒ check the circulatory system by means of contrast enhancers in the presence of ultrasound (Sboros et al. 2002, Frinking & de Jong, Postema et al., Ultrasound Med. Bio. 1998, 2004)

- Sonoporation ⇒ reinforcement of drug delivery to nearby cells that stretch open by oscillating contrast agents
  (Marmottant & Hilgenfeldt, Nature 2003)

- Micro-bubbles act as vectors for drug or gene delivery to targeted cells
  (Klibanov et al., adv. Drug Delivery Rev., 1999,
  Ferrara et al. Annu. Rev. Biomed., 2007)

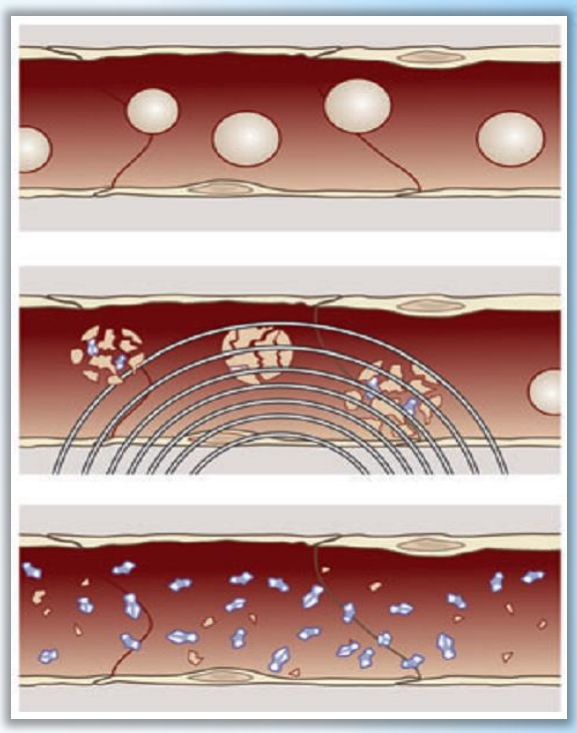

- Need for specially designed contrast agents:
  - Controlled pulsation and break-up for imaging and perfusion measurements
  - Chemical shell treatment for controlled wall adhesion for targeted drug delivery
- Need for models covering a wider range of CA behavior (nonlinear material behavior, shape deformation, buckling, interfacial mass transport etc., compression vs. expansion only behavior, nonlinear resonance frequency-thresholding)
- Need to understand experimental observations and standardize measurements in order to characterize CA's

Asymmetric oscillations of a microbubble near a wall

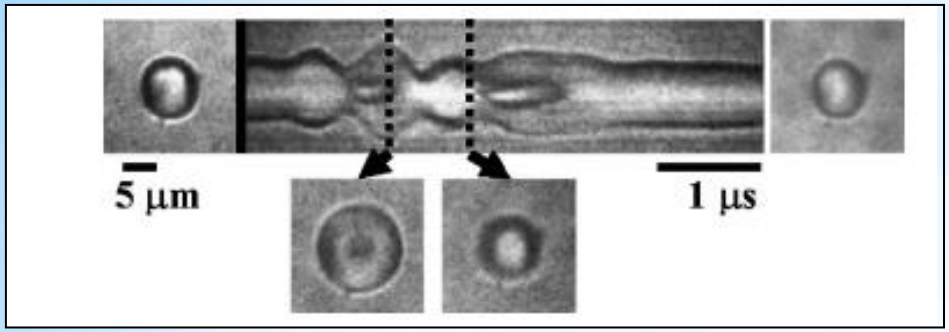

(S. Zhao et al., Applied Physics, 2005)

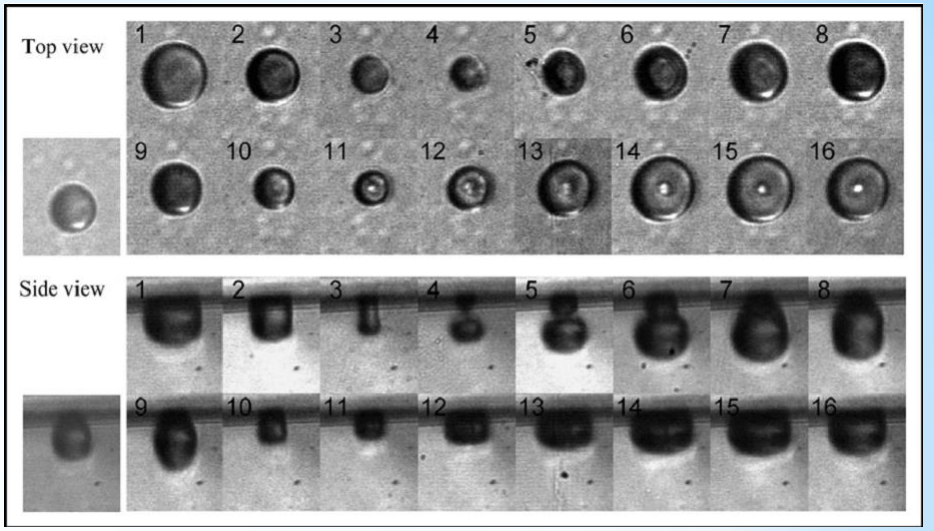

(H. J. Vos et al., Ultrasound in Med. & Biol., 2008)

- Experiments have shown that the presence of a nearby wall affects the bubble's oscillations. In particular its maximum expansion
- Asymmetric oscillations, toroidal bubble shapes during jet inception have been observed
- The bubble oscillates asymmetrically in the plane normal to the wall, while it oscillates symmetrically in the plane parallel to the wall (i.e. deformation has an orientation perpendicular to the wall)

Axisymmetric Pulsations

$$P'_{\infty}(t') = P'_{st}\left[1+\varepsilon\sin\left(\omega_f t'\right)\right],\quad \omega_f = 2\pi\nu_f$$

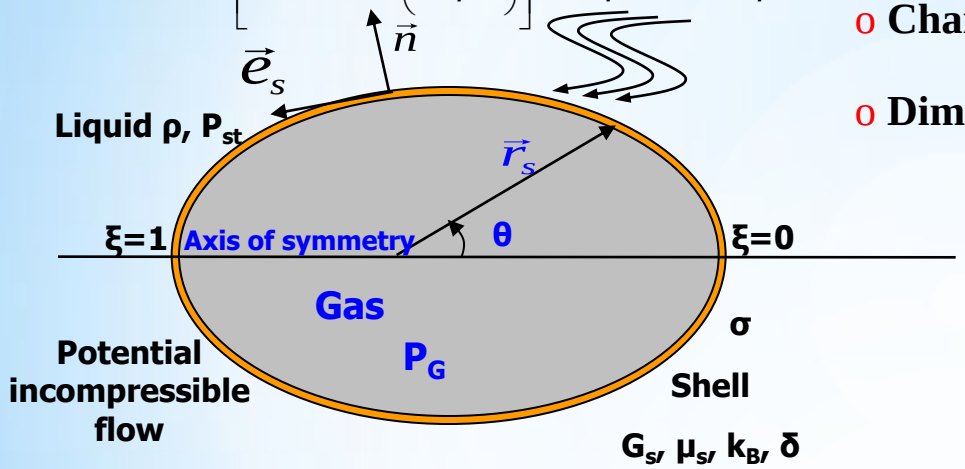

$G_{S,2d}=\delta G_S$

- Characteristic space and time scales: $R_{Eq},\ \sqrt{\rho R_{Eq}^3 / G_{S,2d}}$
- Dimensionless parameters:

$$\omega_f = \frac{\omega'_f}{\sqrt{G_{S,2d}/\left(\rho R_{Eq}^3\right)}} \qquad P = \frac{P_{St}}{\rho G_{S,2d}^2 / R_{Eq}^2}, \qquad We = \frac{G_{S,2d}}{\sigma}$$

$$\mathrm{Re}_l = \sqrt{\frac{\rho G_{S,2d} R_{Eq}}{\mu_l^2}} \qquad B = \frac{k_B}{G_{S,2d} R_{Eq}^2} \qquad \mathrm{Re}_s = \sqrt{\frac{\rho G_{S,2d} R_{Eq}^3}{\mu_S^2}}$$

- Axisymmetry
- Ideal, irrotational flow of high Reynolds number
- Incompressible surrounding fluid with a sinusoidal pressure change in the far field
- Ideal gas in the microbubble undergoing adiabatic pulsations
- Very thin viscoelastic shell whose behavior is characterized by the constitutive law (e.g. Hooke, Mooney-Rivlin or Skalak)
- The shell exhibits bending modulus that determines bending stresses along with curvature variations
- Shell parameters: area dilatation modulus $\chi=3G_s\delta$, dilatational viscosity μ_s, degree of softness b for strain softening shells or area compressibility C for strain hardening ones and the bending modulus k_B

- **Shell viscosity dominates liquid viscosity, $Re_s << Re_l$ and we can drop viscous stresses on the liquid side**
- **Therefore the tangential force balance is satisfied on the shell with the viscous and elastic stresses in the shell balancing each other**

❖ **Force balance on the bubble's interface:**

$$\vec{r} = \vec{r}_s : \left(-P_L \underline{\underline{I}} + \frac{1}{\mathrm{Re}_L} \underline{\underline{X}} \right) \cdot \vec{n} + P_G \vec{n} = \frac{2k_m}{We} \vec{n} + \overrightarrow{\Delta F} = \frac{\left(\vec{\nabla}_s \cdot \vec{n} \right) \vec{n}}{We} + \overrightarrow{\Delta F},$$

$$\overrightarrow{\Delta F} = \Delta F_n \vec{n} + \Delta F_t \vec{e}_s = -\vec{\nabla}_s \cdot \underline{\underline{T}}, \quad \underline{\underline{T}} = \underline{\underline{\tau}}_{El} + \vec{q}\vec{n} + \underline{\underline{\tau}}_{Vis}$$

$\vec{\nabla}_s$: **Surface gradient,** $\underline{\underline{T}}$: **Stress tensor**

$\underline{\underline{\tau}}_{El}$, $\underline{\underline{\tau}}_{vis}$: **Elastic and viscous stress tensors**

$\vec{q}\vec{n}$: **Transverse shear tensor due to bending moments**

❖ **Torque balance on the bubble's interface:**

$\vec{\mathbf{q}} = \vec{\nabla}_s \cdot \underline{\underline{\mathbf{m}}} \cdot (\underline{\underline{\mathbf{I}}} - \vec{\mathbf{n}}\vec{\mathbf{n}})$, $\underline{\underline{\mathbf{m}}}$: **Tensor of bending moments**

Shell Constitutive Laws – Isotropic Tension

- **Linear behavior ⇒ Hooke's law**
  Kelvin–Voigt law with viscous stresses:

$$T_1^H = G_S \frac{1+\nu_s}{1-\nu_s}\left[\lambda^2 - 1\right] = K\left(\lambda^2 - 1\right) = K\frac{\Delta A}{A}$$

K: area dilatation modulus
G_s: shear modulus
ν_s: surface Poisson ratio
$\Delta A/A$: relative area change

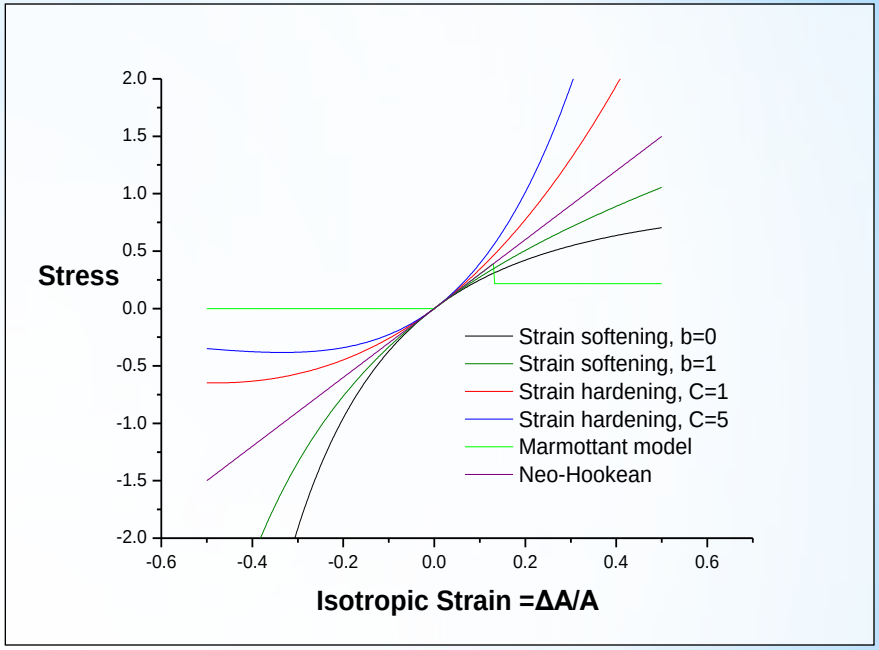

- **Strain softening material (e.g. lipid monolayer)**
  2D Mooney–Rivlin law:

$$T_1^{MR} = \frac{G_{MR}\left(\lambda^4 + \lambda^2 + 1\right)}{\lambda^6}\left[\lambda^2 - 1\right]\left[\Psi + \lambda^2\left(1-\Psi\right)\right], \quad 0 \le \Psi \le 1$$

Ψ=1-b : degree of smoothness

- **Strain hardening material (e.g. red blood-cell membrane that consist of a lipid bilayer)**
  Skalak law:

$$T_1^{SK} = G_{SK}\left[\lambda^2 - 1\right]\left[1 + C\lambda^2\left(1+\lambda^2\right)\right], \quad 1 \le C,$$

C: degree of area compressibility

Phase Diagrams of Polymeric and Lipid Shells

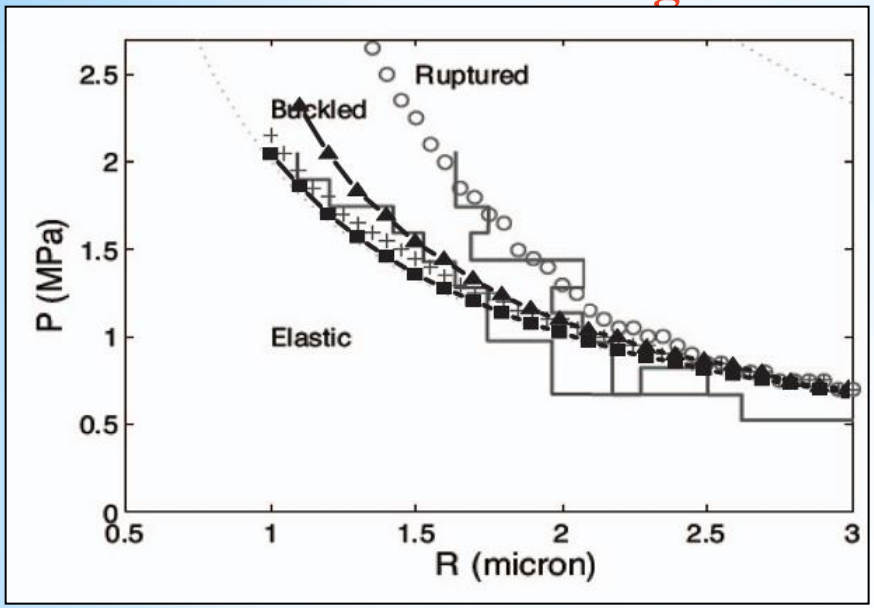

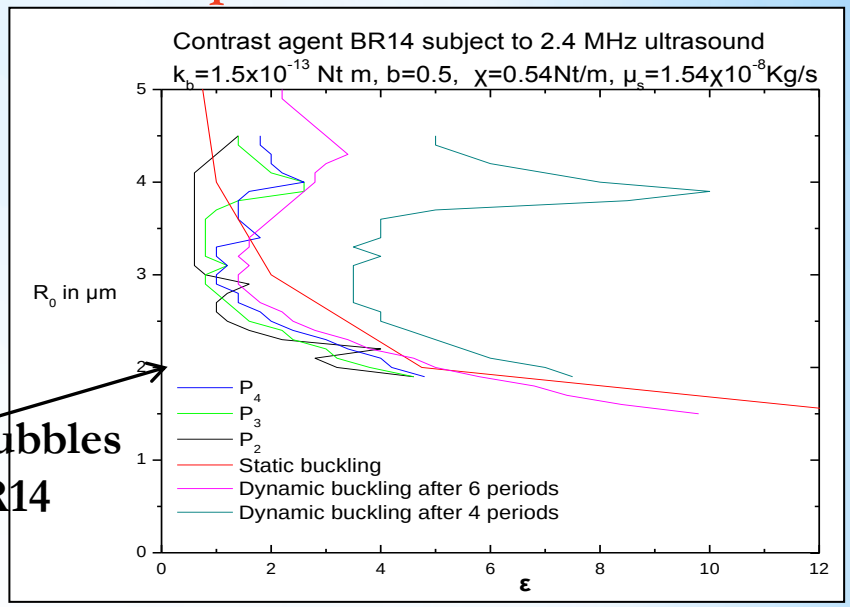

Gas bubbles BR14

- Lower and upper solid lines -> threshold for buckling and transient break-up based on experiments (Bouakaz et al. 2005)
- Lower dotted line, crosses and solid squares -> buckling threshold obtained via static stability, finite element analysis and surface evolver
- Upper dotted line -> static rupture criterion due to stretching at expansion (too high)
- Open circles -> transient break-up based on the revised Marmottant model (requires unrealistically large shell thickness)
- Solid triangles -> Threshold of dynamic buckling based on linear stability and simulations

Parametric excitation of shape modes takes place at lower amplitudes than those required for dynamic and static buckling

Based on the amplitude threshold for shape deformations k_B can be estimated

The behavior of polymeric shells, large area dilatation, conforms with the concept of a viscoelastic solid with stretching and bending stiffness

Parametric Stability – Resonance

$$R_{eq} = 3.6\ \mu m,\ G_s = 80\ MPa,\ \delta = 1\ nm,\ \mu_s = 20\ Pa \cdot s,\ b = 0,\ \nu = 0.5,$$
$$\rho_l = 998\ {}^{kg}/_{m^3},\ P'_{st} = 101325\ Pa,\ \gamma = 1.07,\ \nu_f = 1.7 MHz,\ K_{BD} = 3.0d-14 Nm$$

Saturation - Harmonic resonance

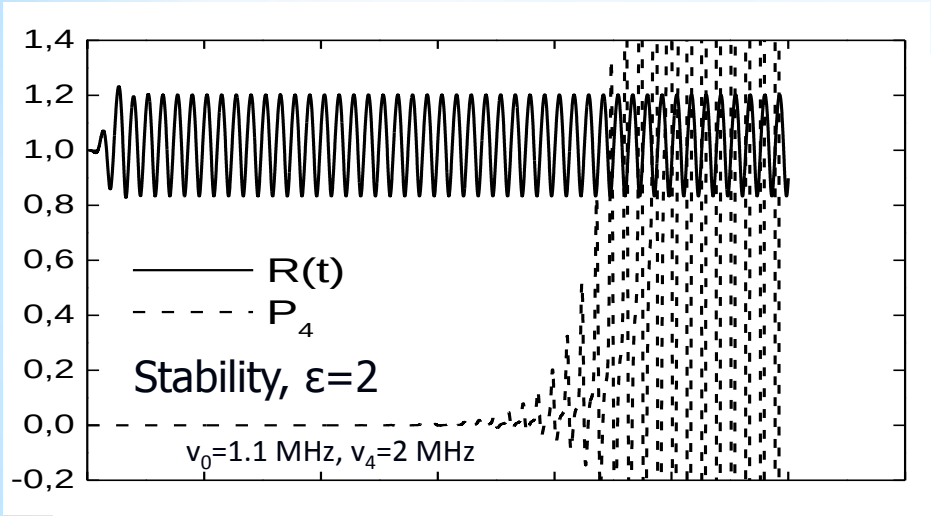

Transient Break-up

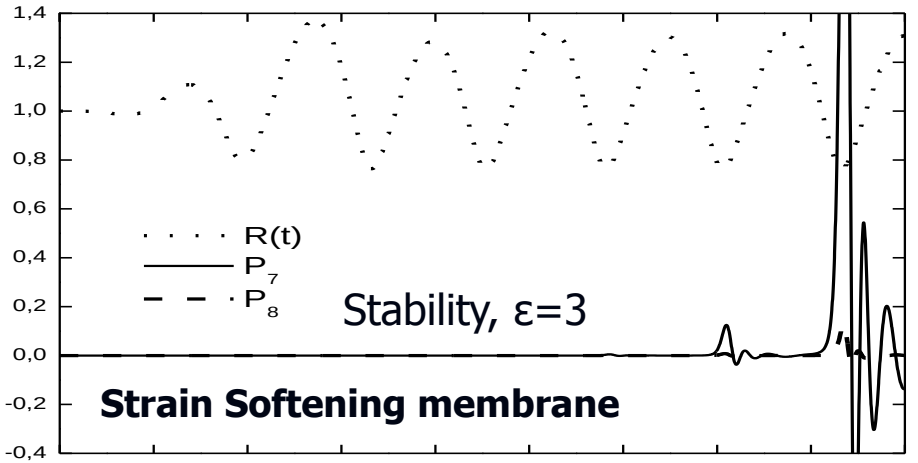

AMPLITUDE

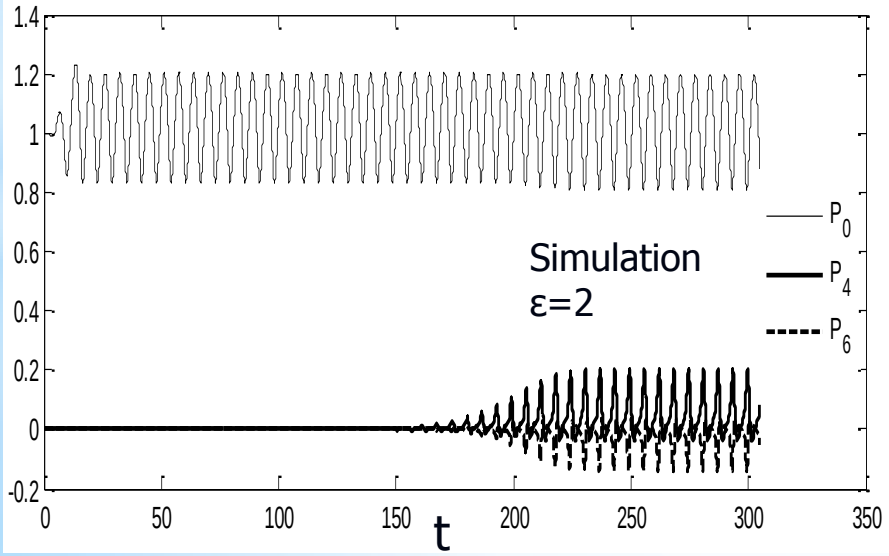

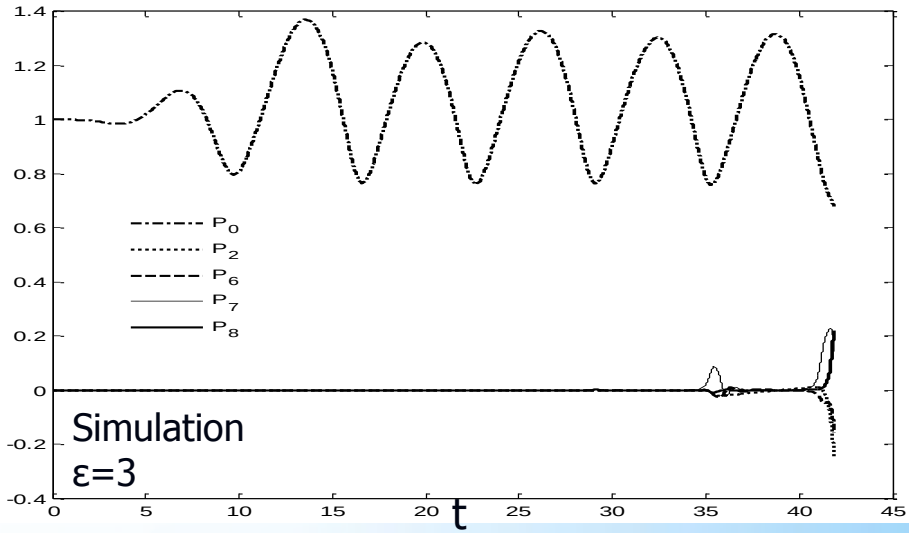

Axisymmetric pulsations of a bubble near a surface

Governing Equations (cylindrical coordinate system)

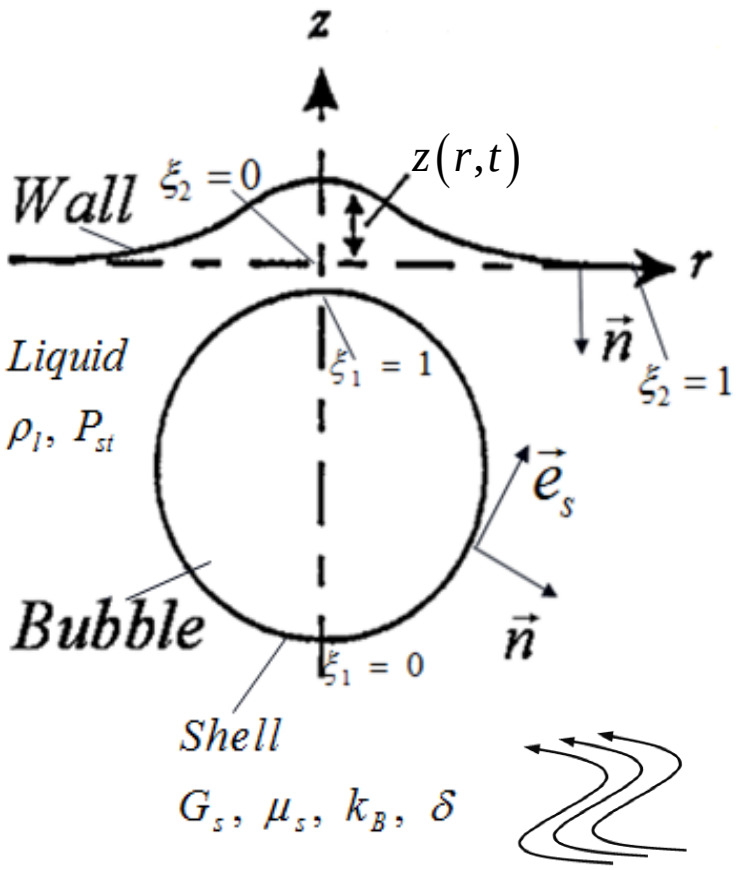

$$P'_\infty(t') = P'_{st}\left[1+\varepsilon\cos\left(\omega_f t'\right)\right],\quad \omega_f = 2\pi\nu_f$$

Kinematic conditions of the bubble's interface:

$$\left.\frac{dr}{dt}\right|_{r_0,z_0} = \frac{\Phi_\xi\cdot r_\xi + \frac{\partial\Phi}{\partial n} z_\xi\cdot\sqrt{r_\xi^2+z_\xi^2}}{r_\xi^2+z_\xi^2},\qquad \left.\frac{dz}{dt}\right|_{r_0,z_0} = \frac{\Phi_\xi\cdot z_\xi - \frac{\partial\Phi}{\partial n} r_\xi\cdot\sqrt{r_\xi^2+z_\xi^2}}{r_\xi^2+z_\xi^2}$$

Dynamic condition on the bubble's interface:

$$\frac{D\Phi}{Dt} = \frac{1}{2}\left[\left(\frac{\partial\Phi}{\partial n}\right)^2 + \frac{\Phi_\xi^2}{r_\xi^2+z_\xi^2}\right] + P_\infty - P_G + \frac{2k_m}{We} + \Delta F_n,\qquad k_m = \vec{\nabla}_s\cdot\vec{n}$$

Boundary conditions due to axisymmetry:

$$\frac{\partial z}{\partial\xi} = \frac{\partial\Phi}{\partial\xi} = \frac{\partial^2\Phi}{\partial\xi\partial n} = \frac{\partial^2 r}{\partial\xi^2} = 0 \qquad \text{στο } \xi_1 = 0,\ 1 \quad (\text{i.e. } r = 0)$$

Boundary integral equation of the interface:

$$\Phi(r_0,z_0,t) = \int_{S_b}\frac{\partial\Phi}{\partial n}(r,z,t)G(r_0,z_0,r,z)\,dS_b -$$

$$-\int_{S_b}\left[\Phi(r,z,t)-\Phi(r_0,z_0,t)\right]\frac{\partial G}{\partial n}(r_0,z_0,r,z)\,dS_b +$$

$$+\int_{S_w}\frac{\partial\Phi}{\partial n}(r,z,t)G(r_0,z_0,r,z)\,dS_w - \int_{S_w}\Phi(r,z,t)\frac{\partial G}{\partial n}(r_0,z_0,r,z)\,dS_w$$

Governing Equations (cont.)

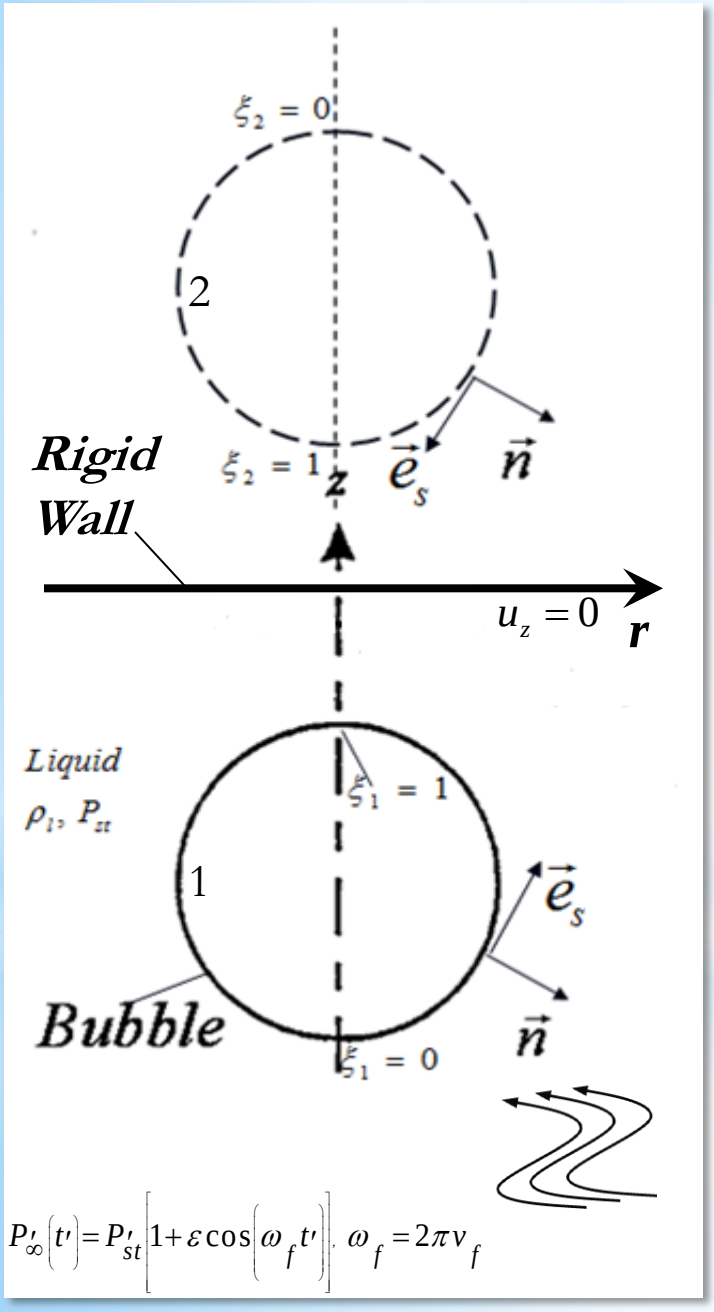

1st assumption: Surface as a rigid wall:

In this case a second symmetric bubble with respect to r-axis is considered

We calculate the two kinematic conditions and dynamic condition by means of Finite Element Method in order to compute the position of bubble's interface and the velocity potential. Owing to symmetry, we solve only for the first bubble.

We calculate the boundary integral equation by means of Boundary Element Method in order to compute the normal velocity of the interfaces:

$$\Phi(r_0,z_0,t) = \int_{S_{b1}} \frac{\partial\Phi}{\partial n}(r,z,t)\,G(r_0,z_0,r,z)\,dS_{b1} -$$

$$-\int_{S_{b1}} \left[\Phi(r,z,t)-\Phi(r_0,z_0,t)\right]\frac{\partial G}{\partial n}(r_0,z_0,r,z)\,dS_{b1} +$$

$$+\int_{S_{b2}} \frac{\partial\Phi}{\partial n}(r,z,t)\,G(r_0,z_0,r,z)\,dS_{b2} - \int_{S_{b2}} \Phi(r,z,t)\frac{\partial G}{\partial n}(r_0,z_0,r,z)\,dS_{b2}$$

where (r_0,z_0): the field point

Governing Equations (cont.)

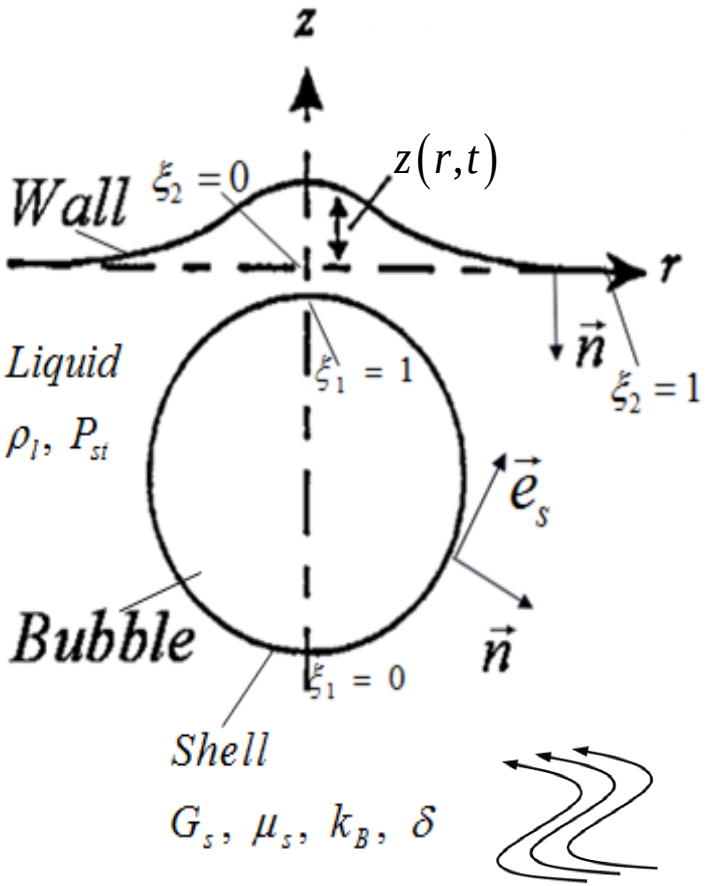

$$P'_\infty(t') = P'_{st}\left[1+\varepsilon\cos\left(\omega_f t'\right)\right],\quad \omega_f = 2\pi\nu_f$$

2nd assumption: Free surface

The kinematic conditions are the same for the surface

Dynamic condition on the surface/liquid interface:

$$\frac{D\Phi}{Dt} = \frac{1}{2}\left[\left(\frac{\partial\Phi}{\partial n}\right)^2 + \frac{\Phi_\xi^2}{r_\xi^2 + z_\xi^2}\right] + P_\infty - P_{st} + \frac{2k_m}{We},\quad k_m = \vec{\nabla}_s \cdot \vec{n}$$

Boundary conditions due to axisymmetry :

$$\frac{\partial z}{\partial\xi} = \frac{\partial\Phi}{\partial\xi} = \frac{\partial^2\Phi}{\partial\xi\partial n} = \frac{\partial^2 r}{\partial\xi^2} = 0 \qquad \text{στο } \xi_2 = 0 \text{ (i.e. r = 0)}$$

In the far field:

$$\frac{\partial^2 r}{\partial\xi^2} = \frac{\partial z}{\partial\xi} = \frac{\partial\Phi}{\partial\xi} = \frac{\partial\Phi}{\partial n} = 0 \qquad \text{στο } \xi_2 = 1 \text{ (i.e. r} = 20\cdot R_0)$$

3rd assumption: Surface as an elastic wall

We consider an elastic wall of very small thickness

Similar approach as in the case of bubble's shell (i.e. modeling via classical shell theory)

Dynamic condition on the surface/liquid interface:

$$\frac{D\Phi}{Dt} = \frac{1}{2}\left[\left(\frac{\partial\Phi}{\partial n}\right)^2 + \frac{\Phi_\xi^2}{r_\xi^2 + z_\xi^2}\right] + P_\infty - P_{tr} + \frac{2k_m}{We} + \Delta F_n,\quad k_m = \vec{\nabla}_s \cdot \vec{n}$$

Numerical Methodology

Algorithm

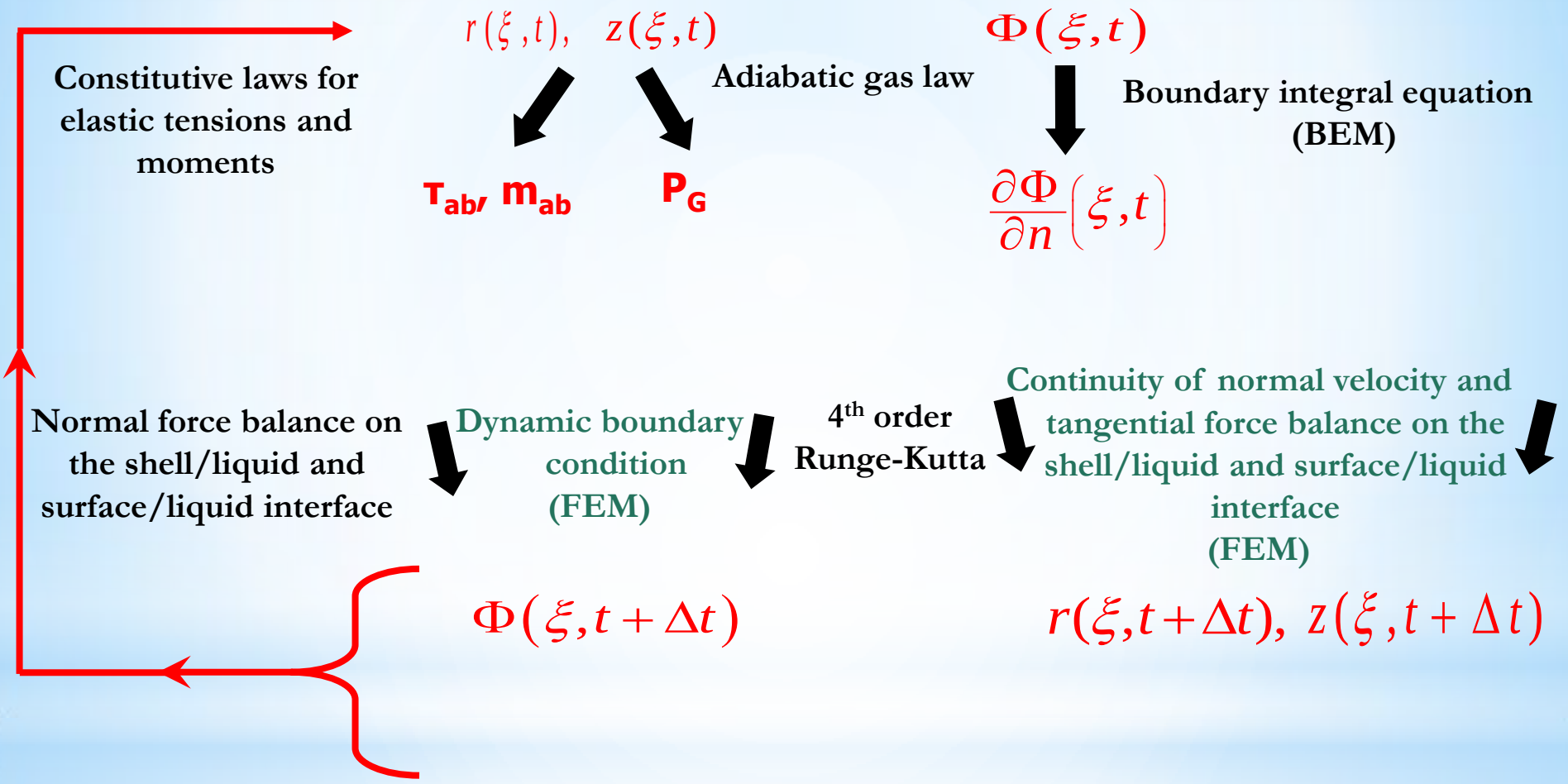

Numerical Results

Benchmark – Interaction between two similar uncoated bubbles:

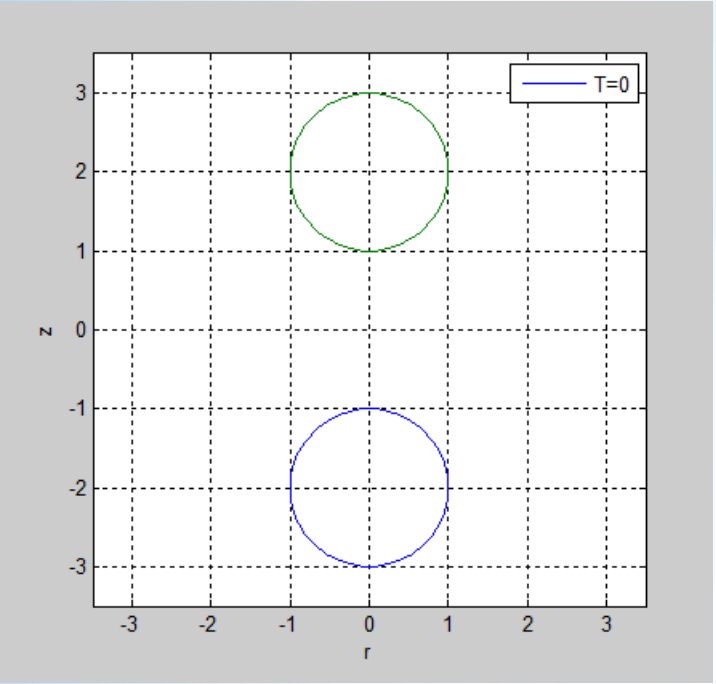

- Actually, this is the case of an uncoated bubble near a rigid wall (i.e. the 1st assumption) and how it responds to a step change in pressure in the far field
- The position of the interface (i.e. r(t) , z(t)) is computed via the continuity of normal and tangential velocity:

$$\frac{\partial r}{\partial t}\cdot\frac{\partial z}{\partial s}-\frac{\partial z}{\partial t}\cdot\frac{\partial r}{\partial s}=\frac{\partial \Phi}{\partial n} \qquad \frac{\partial r}{\partial t}\cdot\frac{\partial r}{\partial s}+\frac{\partial z}{\partial t}\cdot\frac{\partial z}{\partial s}=\frac{\partial \Phi}{\partial s}$$

- In the dynamic condition the elastic stresses are excluded in the absence of coating:

$$\frac{D\Phi}{Dt}=\frac{1}{2}\left[\left(\frac{\partial \Phi}{\partial n}\right)^2+\frac{\Phi_\xi^2}{r_\xi^2+z_\xi^2}\right]+P_\infty-P_{st}+\frac{2k_m}{We},\quad k_m=\vec{\nabla}_s\cdot\vec{n}$$

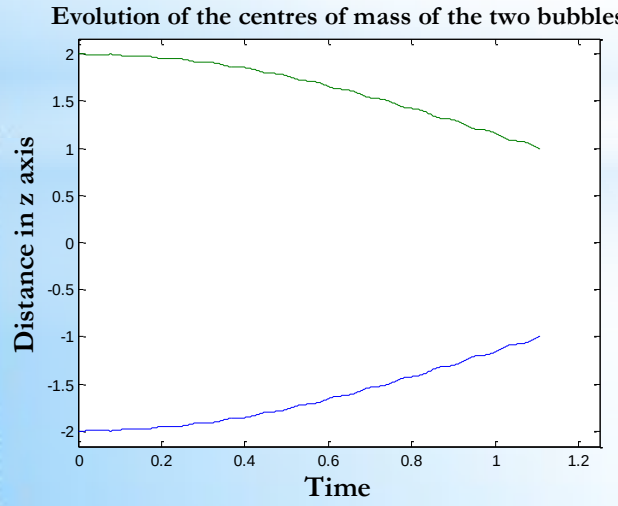

- The results are very close to those in the literature (N. A. Pelekasis & J. A. Tsamopoulos, 1991)

Numerical Results (cont.)

Interaction between two similar coated bubbles:

- **This is the case of a coated bubble near a rigid wall (i.e. the 1st assumption) and how it responds to a step change in pressure in the far field**
- **The position of the interface (i.e. r(t) , z(t)) is computed via the continuity of normal velocity and the tangential force balance:**

$$\frac{\partial r}{\partial t}\cdot\frac{\partial z}{\partial s}-\frac{\partial z}{\partial t}\cdot\frac{\partial r}{\partial s}=\frac{\partial \Phi}{\partial n} \qquad \frac{\partial \tau_{ss}}{\partial s}+\frac{1}{r}\cdot\frac{\partial r}{\partial s}\left(\tau_{ss}-\tau_{\varphi\varphi}\right)+k_s\cdot q=0$$

- **Dynamic condition on the bubble's interface contains elastic stresses:**

$$\frac{D\Phi}{Dt}=\frac{1}{2}\left[\left(\frac{\partial \Phi}{\partial n}\right)^2+\frac{\Phi_\xi^2}{r_\xi^2+z_\xi^2}\right]+P_\infty-P_G+\frac{2k_m}{We}+\Delta F_n, \quad k_m=\vec{\nabla}_s\cdot\vec{n}$$

- **In this case, coupling of continuity of normal velocity with the tangential force balance fails due to growth of short waves**

- **We also tried to compute z(t) via the kinematic condition in z-direction and r(t) via tangential force balance, with similar problems**

$$\left.\frac{dz}{dt}\right|_{r_0,z_0}=\frac{\Phi_\xi\cdot z_\xi-\frac{\partial \Phi}{\partial n}r_\xi\cdot\sqrt{r_\xi^2+z_\xi^2}}{r_\xi^2+z_\xi^2} \qquad \frac{\partial \tau_{ss}}{\partial s}+\frac{1}{r}\cdot\frac{\partial r}{\partial s}\left(\tau_{ss}-\tau_{\varphi\varphi}\right)+k_s\cdot q=0$$

Ongoing work

- ✓ **The assumption of a local spherical coordinate system with its origin at the centre of mass of the microbubble is to be adopted**
- ✓ **The coupling of continuity of normal velocity and tangential force balance in spherical coordinate system is to be tested**

Conclusions

- Nonlinear shell properties, e.g. strain softening vs. strain hardening membrane material, significantly affect contrast agent response
- Allowing for bending elasticity shape deformation and buckling are captured. Bending elasticity is independent from area dilatation modulus due to non-isotropy of the membrane
- **Polymeric** shells follow a **neo-Hookean** behavior - **Lipid monolayer** shells exhibit a **strain softening behavior** (they become softer at expansion as the area density of the monolayer decreases) – **Lipid bilayer** shells exhibit **strain hardening** behavior (they become softer at compression)
- Dynamic buckling (equivalent to Rayleigh-Taylor instability for free bubbles) occurs exponentially fast. Polymeric shells mainly exhibit this type of dynamic behavior that can be explained by coupling classical shell theory with potential theory for the liquid motion

Conclusions (cont.)

- Shell viscosity constitutes the main damping mechanism
- With the available modeling tools a number of dynamic effects exhibited by contrast agents is understood and captured, e.g. resonance frequencies, abrupt vibration onset, rich harmonic content, expansion and compression only behavior
- Mode saturation is captured above the stability threshold (supercritical growth) for parametric excitation -- Growth of unstable modes occurs mostly during compression - As the amplitude increases towards the threshold for dynamic buckling transient break-up takes place

Future work

- ✓ Parametric study of the distance between the bubble and the surface as well the properties of the latter in the backscatter signal

Acknowledgements

This research has been co-financed by the European Union (European Social Fund - ESF) and Greek national funds through the Operational Program "Education and Lifelong Learning" of the National Strategic Reference Framework (NSRF) - Research Funding Program: Aristeia I. Investing in knowledge society through the European Social Fund.

Thanks for your attention

Questions